



# Synthesis of boron/nitrogen substituted carbons for aqueous asymmetric capacitors

Timothy Tomko<sup>a</sup>, Ramakrishnan Rajagopalan<sup>b,\*</sup>, Parvana Aksoy<sup>c</sup>, Henry C. Foley<sup>d</sup>

<sup>a</sup> Energy and Mineral Engineering, The Pennsylvania State University, University Park, PA 16802, United States

<sup>b</sup> Materials Research Institute, The Pennsylvania State University, 270 MRL Bldg., University Park, PA 16802, United States

<sup>c</sup> Energy Institute, The Pennsylvania State University, University Park, PA 16802, United States

<sup>d</sup> Department of Chemical Engineering, The Pennsylvania State University, University Park, PA 16802, United States

## ARTICLE INFO

### Article history:

Received 16 October 2010

Received in revised form 26 January 2011

Accepted 18 March 2011

Available online 2 April 2011

### Keywords:

Asymmetric electrochemical capacitor

Boron/nitrogen carbon

Coal tar pitch

Manganese dioxide

Polyborazylene

## ABSTRACT

Boron/nitrogen substituted carbons were synthesized by co-pyrolysis of polyborazylene/coal tar pitch blends to yield a carbon with a boron and nitrogen content of 14 at% and 10 at%, respectively. The presence of heteroatoms in these carbons shifted the hydrogen evolution overpotential to  $-1.4$  V vs Ag/AgCl in aqueous electrolytes, providing a large electrochemical potential window ( $\sim 2.4$  V) as well as a specific capacitance of  $0.6$  F/m<sup>2</sup>. An asymmetric capacitor was fabricated using the as-prepared low surface area carbon as the negative electrode along with a redox active manganese dioxide as the positive electrode. The energy density of the capacitor exceeded 10 Wh/kg at a power density of 1 kW/kg and had a cycle life greater than 1000 cycles.

© 2011 Elsevier Ltd. All rights reserved.

## 1. Introduction

Carbon has been used extensively as an electrode material in symmetric and asymmetric electrochemical capacitors for both aqueous and non-aqueous electrolytes [1–4]. The advantages of using carbon as an electrode material in electrochemical capacitors include: excellent cycle life, large coulombic efficiencies and high power densities. Traditionally, carbons with a high surface area and mean pore size close to 1–3 nm have been used to make symmetric capacitors with energy densities in the order of 5 Wh/kg [5,6]. The narrow pore size distribution of these carbons can also lead to electrochemical hydrogen storage making them feasible to be used as negative electrodes in aqueous asymmetric electrochemical capacitors with energy densities greater than 20 Wh/kg and cell voltage as high as 2.0 V [7–9].

The specific capacitance of the carbon in aqueous electrolytes can be improved further by incorporating heteroatoms such as oxygen, nitrogen and boron in the carbon framework due to favorable redox reactions. It was shown that addition of oxygen functional groups such as quinone/hydroquinone groups increases the specific capacitance of the carbon significantly [10]. Similarly, nitrogen

functional groups such as pyridonic groups can result in a pseudo-capacitive response in aqueous electrolytes [11,12]. Beguin et al. showed that the decoration of carbon nanotubes with nitrogen functional groups can lead to very high specific capacitance per unit area [12]. More recently, pseudocapacitive responses in boron substituted carbons have also been demonstrated. The mechanism of improved capacitances in heteroatom doped carbons can be attributed to several reasons including faradaic reactions, improved wettability, space charge layer capacitance and conductivity of the material [13,14]. Kyotani et al. recently showed that the improved specific capacitance was primarily due to faradaic reactions by evaluating the performance of boron and nitrogen doped carbons deposited on an anodized alumina template [15].

There have been very few studies on the electrochemical activity of boron/nitrogen substituted carbons (BCN). The presence of both boron and nitrogen in the carbon domains can result in a significant increase of the interfacial capacitance due to possible redox reactions. Recently, the electrochemical properties of high surface area BCN were investigated and it was shown that the specific capacitance of these carbons can be as high as 300 F/g [16]. In this investigation, we report a novel synthetic route to produce BCN materials with boron and nitrogen content as high as 14 at%. The synthesized carbons show strong electroadsorption of protons and are very promising candidates for use as negative electrodes in aqueous asymmetric capacitors.

\* Corresponding author. Tel.: +1 814 863 1880; fax: +1 814 863 8561.  
E-mail address: [rur12@psu.edu](mailto:rur12@psu.edu) (R. Rajagopalan).

## 2. Experimental

### 2.1. Synthesis and characterization of electrode materials

Coal tar pitch (CTP) was dissolved in THF and the soluble fraction of the pitch was recovered through filtration followed by evaporation of excess THF. The filtrate was then mixed with polyborazylene, 1:1 (w/w), and co-dissolved in THF. The blend was co-precipitated in n-pentane, filtered and pyrolyzed at 800 °C under an argon atmosphere. The pyrolyzed carbon was then washed, filtered and dried to constant weight [17,18]. CTP and polyborazylene were obtained from Koppers Inc. and Boroscience Inc., respectively.

Synthesis of high surface area MnO<sub>2</sub> was adapted from a procedure described by Subramanian et al. [19]. To produce the high surface area manganese dioxide (MnO<sub>2</sub>), 0.5 g of potassium permanganate (KMnO<sub>4</sub>) was dissolved in 10 mL of water in a small beaker, while 50 mg of Triton X-100 surfactant, 20 mL of hexane, and 5 mL of methanol were mixed in a separate beaker. The surfactant mixture was added in a dropwise fashion to the aqueous KMnO<sub>4</sub>. The resultant mixture was stirred and ultrasonicated for 10 min. The solution was filtered and rinsed thoroughly several times to ensure no surfactant remained in the sample. The solid residue was then dried at 100 °C to constant weight.

In order to compare the electrochemical performance of the synthesized carbons, high surface area activated carbon (AC) derived from the same source (CTP) with a surface area of 1700 m<sup>2</sup>/g was prepared using the method described previously [17,18].

XPS measurements (Kratos Analytical Axis ultra Instrument, Chestnut Ridge, NY) were done to determine the amount of carbon, nitrogen, oxygen and boron present in the BCN sample. Powder X-ray diffraction was used to confirm the composition of the synthesized BCN using a Scintag X2 powder Diffractometer using a CuK $\alpha$  radiation. Acquisition conditions were 35 kV and 30 mA.

### 2.2. Electrochemical characterization

#### 2.2.1. Three-electrode electrochemical testing

The electrodes were prepared by combining 0.085 g of active material (BCN or AC), 0.01 g Teflon binder and 0.005 g of acetylene black. The resultant powder was then dispersed in 1 mL of THF and the solution was ultrasonicated for 20 min. 2 mg of the resultant slurry was applied to 1 cm<sup>2</sup> of carbon fiber mat (supplied by Technical Fibres Inc.) and blown dry to constant weight. All electrochemical measurements were done using a 263A Potentiostat/Galvanostat. The active electrode materials were tested individually as the working electrodes using a platinum wire as a counter electrode and Ag/AgCl as a reference electrode in aqueous 2 M calcium chloride (CaCl<sub>2</sub>). The pH of the aqueous electrolyte solution was adjusted to 7 using dilute acetic acid and the cyclic voltammograms were measured at a scan rate of 10 mV/s using a scan range of -1 V to 0.8 V for AC and -1.4 V to 1 V for BCN vs Ag/AgCl, respectively.

#### 2.2.2. Two electrode measurements

Electrode materials namely AC and BCN were prepared similar to the 3-electrode measurements. 0.07 g of manganese oxide, 0.01 g of Teflon binder, and 0.02 g of acetylene black were used to make the MnO<sub>2</sub> electrode. Prior to assembly of the cell, the electrode materials, as well as a Celgard 3501 membrane, were soaked in aqueous 2 M CaCl<sub>2</sub> electrolyte, under vacuum, for 30 min. Tantalum foils were used as the current collectors for both the electrodes. The two-electrode capacitor was assembled together such that AC or BCN was used as the negative electrode and MnO<sub>2</sub> was used as the positive electrode. The cell was then soaked in the aqueous

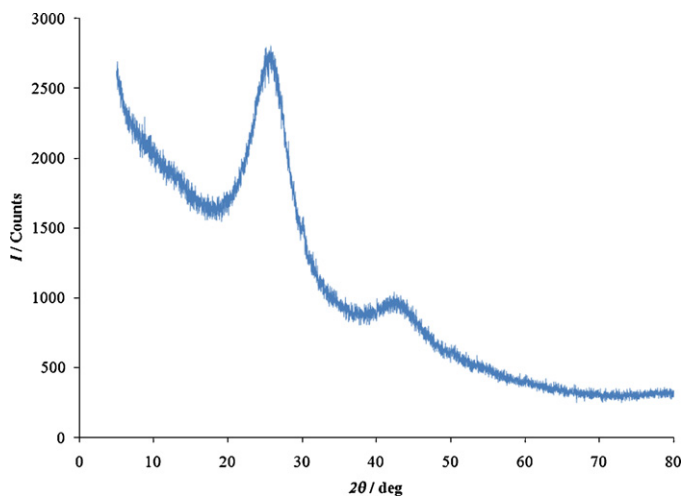


Fig. 1. XRD of synthesized BCN powder.

electrolyte and tested using cyclic voltammetry, electrochemical impedance spectroscopy and constant current charge/discharge cycling. Cyclic voltammetry was done using a scan range of 0–1 V for the symmetric AC capacitor and 0.1–2.4 V for BCN/MnO<sub>2</sub> at a scan rate of 10 mV/s for 100 cycles. The mass of AC, MnO<sub>2</sub> and BCN electrodes were 2 mg, 2 mg and 7 mg, respectively. The EIS measurements were done using a model 5210 Lock-in amplifier coupled with 263A Potentiostat/Galvanostat. An ac perturbation of 10 mV was applied at open circuit voltage conditions. The frequency of the ac perturbation was varied from 10<sup>5</sup> Hz to 10<sup>-3</sup> Hz. The equivalent series resistance (ESR) of the cell was computed using the impedance data measured at 100 Hz. The obtained Nyquist plot was also fitted to an equivalent circuit model using ZView software. Galvanostatic charge/discharge cycling was done by applying a load current density ranging from 70 mA/g to 1.4 A/g for symmetric AC and 130 mA/g to 2.5 A/g for BCN/MnO<sub>2</sub> and the cycle life was determined up to 1000 cycles. Specific capacitances, energy densities and power densities were computed from the discharge curves.

## 3. Results

### 3.1. Characterization of synthesized BCN

XRD of BCN prepared by pyrolysis of a polyborazylene/CTP blend showed two broad peaks positioned at 26° and 42° corresponding to 002 and 200 reflections, respectively (Fig. 1). The d-spacing of the 002 plane was 3.45 Å indicating highly disordered carbon with L<sub>c</sub> in the order of 1–2 nm. The elemental composition of BCN was determined using XPS as shown in Table 1. The stoichiometric ratio of the synthesized compound was B<sub>1.4</sub>C<sub>5.1</sub>N<sub>0.2</sub> with boron

Table 1  
Elemental composition and binding energy, as determined by XPS, of BCN powders.

Element	Composition (at%)	Components	Binding energy (eV)
B1s	14.24	B–N or B–C	191.0
		B–O	192.4
C1s	53.61	C–C	285
		C–N	286.2
		C=O	287
N1s	10.46	B–N or pyridinic N	398.5
		C–N	399.4
		Quaternary N	400
O1s	21.22	C=O	532

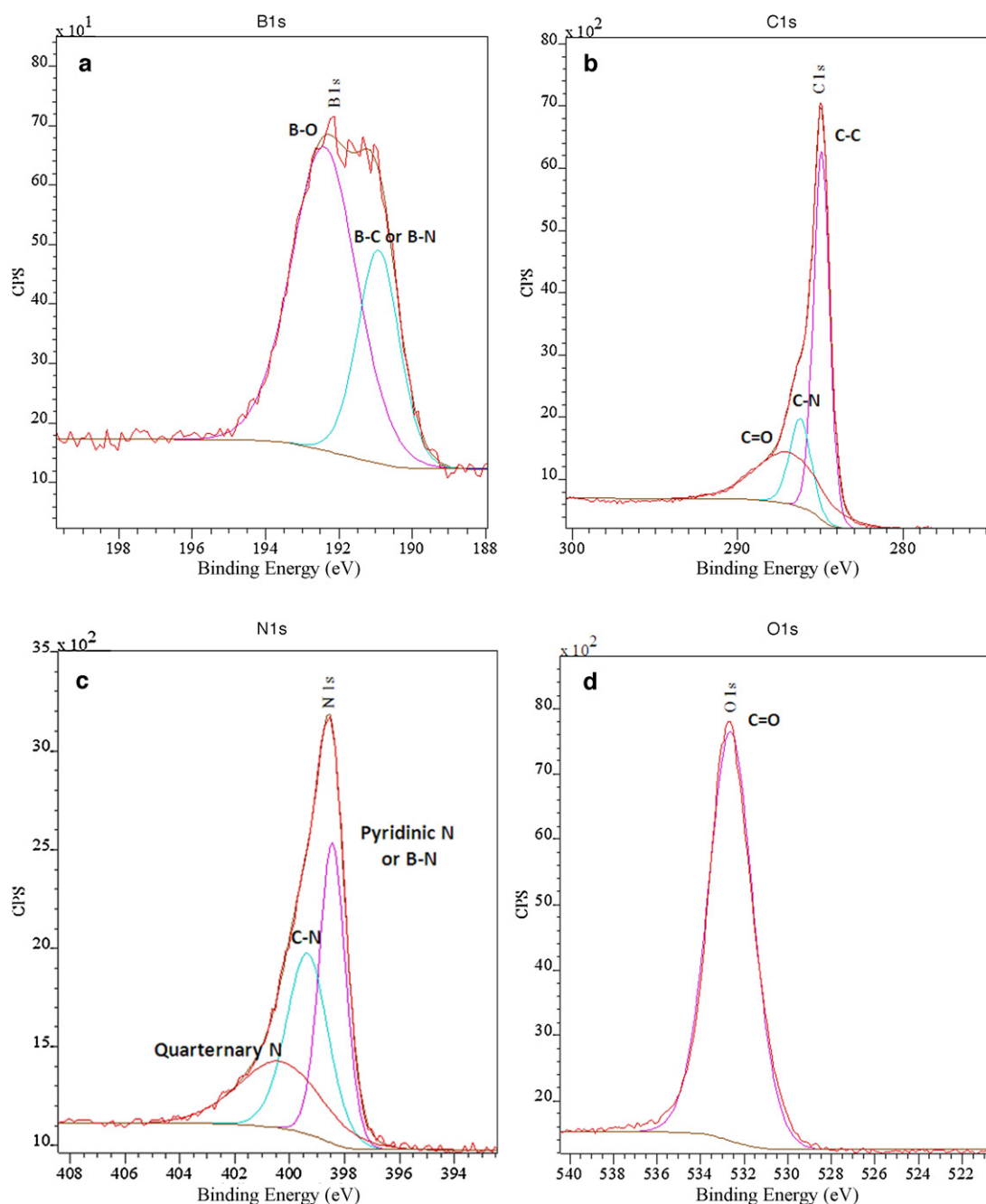


Fig. 2. Deconvoluted high resolution XPS spectrum of BCN: (a) B1s, (b) C1s, (c) N1s, and (d) O1s.

and nitrogen content as high as 14.24 at% and 10.46 at%, respectively. Fig. 2a–d shows the deconvoluted B1s, C1s, N1s and O1s XPS high resolution spectrum. The B1s spectrum was deconvoluted into two peaks at 191.0 eV and 192.4 eV [20,21]. The origin of the 191.0 eV peak could be either due to B–N or B–C and the presence of a peak at 192.4 eV shows that some of the boron species have been oxidized. N1s was curvefitted into three components centered at 398.5 eV, 399.4 eV and 400.4 eV. The 398.5 eV could be assigned to either B–N or the presence of pyridinic N groups [22]. The peaks at higher binding energies (>399 eV) indicate that the nitrogen was also bonded with carbon. The deconvoluted C1s spectrum show peaks at 285 eV, 286.2 eV and 287 eV corresponding to C–C in polyaromatic domains, C–N and C=O, respectively [23]. O1s spectrum was fitted to a single peak at 532.6 eV assigned to C=O [24].

### 3.2. Three-electrode measurements

Cyclic voltammetry was performed on AC and BCN in aqueous  $\text{CaCl}_2$  at 10 mV/s (Fig. 3). The specific capacitance of the electrode was calculated from the following:

$$C = \frac{Q_a + |Q_c|}{2V\upsilon m} \quad (1)$$

where  $Q_a$  and  $Q_c$  are the anodic and cathodic charges respectively in coulombs,  $V$  is the scan range in volts,  $\upsilon$  is the scan rate in V/s, and  $m$  is the mass of the active material in grams.

The electrochemical potential window was determined based on the hydrogen evolution potential for negative electrode materials (BCN and AC) as the lower limit, while the upper limit was determined by a steep increase in the anodic current due to oxygen

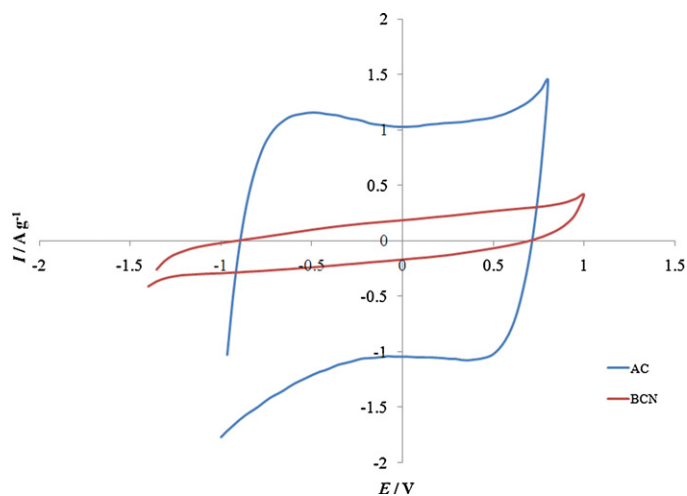


**Fig. 3.** Three-electrode cyclic voltammogram of BCN and AC at a scan rate of 10 mV/s using Ag/AgCl as a reference electrode in aqueous 2 M CaCl<sub>2</sub> electrolyte.

gas evolution. The AC was cycled between  $-1$  V to  $0.8$  V vs Ag/AgCl and showed a specific capacitance of  $75$  F/g. The as-synthesized BCN showed an increased potential range of  $-1.4$  V to  $1$  V vs Ag/AgCl and a specific capacitance of  $30$  F/g. Table 2 compares the specific capacitance per unit area for three different electrode materials. High surface area AC showed a specific capacitance of  $0.04$  F/m<sup>2</sup>, which was indicative of primarily electrostatic interaction due to double layer capacitance [25]. BCN showed a specific capacitance of  $0.60$  F/m<sup>2</sup>, which was substantially higher than double layer response suggesting possible pseudocapacitive contributions. In comparison, redox active MnO<sub>2</sub> had a specific capacitance of  $2.3$  F/m<sup>2</sup>, clearly indicating a pseudocapacitive response.

### 3.3. Two-electrode measurements

Based on the 3-electrode measurements, mass ratio of BCN/MnO<sub>2</sub> was determined by balancing the charge on each electrode. Fig. 4 shows the two-electrode cyclic voltammograms of a symmetric AC cell and an asymmetric BCN/MnO<sub>2</sub> performed at a scan rate of 10 mV/s. The specific capacitance was measured as follows:

$$C = \frac{I}{\nu m} \quad (2)$$

where  $I$  is the anodic or cathodic current in amperes,  $\nu$  is the scan rate in V/s, and  $m$  is the total active mass of both the electrodes in grams.

The gravimetric cell capacitance of both symmetric AC and asymmetric BCN/MnO<sub>2</sub> were very similar ( $\sim 20$  F/g). However, there was a dramatic increase in the cell voltage with the asymmetric BCN/MnO<sub>2</sub> system. The cell voltage can be increased by almost 2.5 times the symmetric AC capacitor.

The ESR values of the symmetric AC and asymmetric BCN/MnO<sub>2</sub> capacitors were  $12$   $\Omega$  and  $15$   $\Omega$ , respectively (Fig. 5). An equivalent circuit was fitted to the impedance spectra as shown in Fig. 5.  $R_1$  corresponds to the sum total of all the series resistances (electronic and solution resistance).  $R_2$  corresponds to the resistive contributions at

**Table 2**  
Specific capacitance (per unit mass and per unit area) of BCN, AC and MnO<sub>2</sub>.

Electrodes	$A$ (m <sup>2</sup> g <sup>-1</sup> )	$C$ (F g <sup>-1</sup> )	$C$ (F m <sup>-2</sup> )
AC	1700	75	0.04
BCN	50	30	0.60
MnO <sub>2</sub>	130	300	2.30

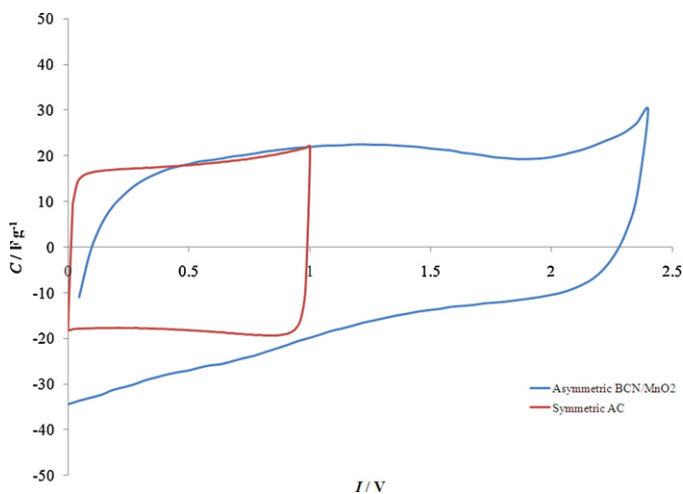


**Fig. 4.** Two-electrode cyclic voltammograms of symmetric AC and asymmetric BCN/MnO<sub>2</sub> capacitors at a scan rate of 10 mV/s in 2 M aqueous CaCl<sub>2</sub> electrolyte.

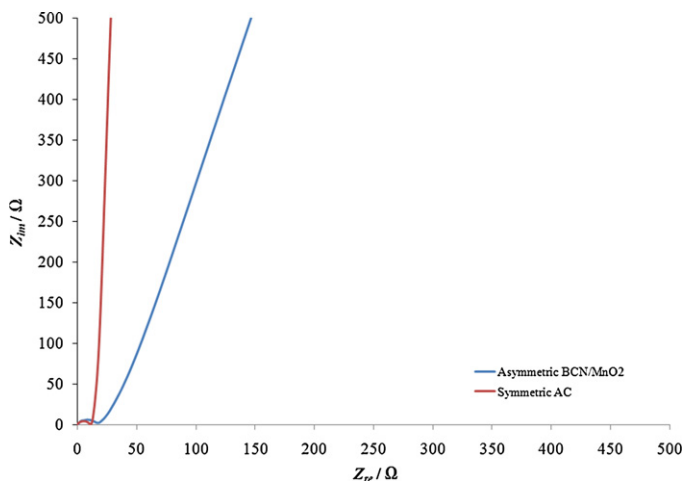


**Fig. 5.** Nyquist plot and equivalent circuit diagram of symmetric AC and asymmetric BCN/MnO<sub>2</sub> systems.

the grain boundary of the electrode materials (charge transfer/grain boundary resistance).  $C_1$  represents the capacitance at each grain boundary layer, while  $CPE_1$  is a constant phase element accounting for the double layer/pseudocapacitive response at each electrode. The values of  $R_1$  and  $C_2$  are high for BCN/MnO<sub>2</sub> due to a large ionic resistance of the low surface area BCN and charge transfer resistance from both BCN and MnO<sub>2</sub> (Table 3). The CPE element was obtained from the fit and its contribution to the overall impedance is as follows:

$$Z = \frac{1}{T(j\omega)^P} \quad (3)$$

where  $Z$  is the impedance in ohm,  $T$  and  $P$  are the CPE parameters, respectively, and  $\omega$  is the angular frequency in rad/s

**Table 3**  
Fitted parameters of the equivalent circuit model for the symmetric AC and asymmetric BCN/MnO<sub>2</sub> systems.

System	$R_1$ ( $\Omega$ )	$R_2$ ( $\Omega$ )	$C_1$ ( $\mu$ F)	CPE1	
				$T$	$P$
AC	1.56	10.85	5.47	0.06	0.98
BCN/MnO <sub>2</sub>	1.26	16.90	10.12	0.06	0.84

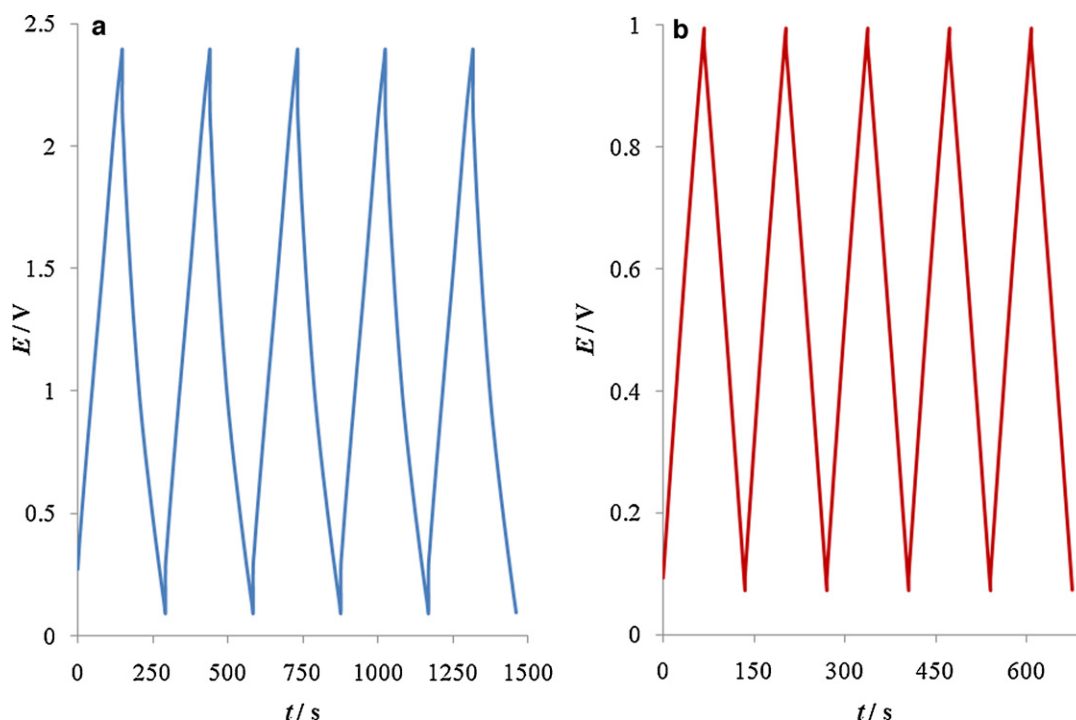


Fig. 6. Constant current charge/discharge curves at a load current density of 250 mA/g (a) asymmetric BCN/MnO<sub>2</sub> and (b) symmetric AC.

As shown in Table 3, the value of  $P$  for AC was 0.98 indicating a highly capacitive behavior while that of BCN/MnO<sub>2</sub> was 0.84 due to its faradaic response.

The constant current charge discharge curves for both BCN/MnO<sub>2</sub> and symmetric AC shows a linear profile indicating a capacitive response (Fig. 6a and b). The specific capacitance was calculated from the discharge curve as follows:

$$C = \frac{i \times \Delta t}{\Delta V} \quad (4)$$

where  $i$  is the specific current density in A/g,  $\Delta t$  is the discharge time in seconds, and  $\Delta V$  is the potential drop during discharge in volts.

The symmetric AC was charged up to 1.0 V while the asymmetric BCN/MnO<sub>2</sub> could be charged to 2.4 V at a load current density of 250 mA/g.

The cycle life performance of the asymmetric BCN/MnO<sub>2</sub> was tested over a period of 1000 cycles. Constant current charge/discharge was performed at a load current density of 250 mA/g (Fig. 7). The specific capacitance of the cell remained stable at approximately 14.5 F/g throughout the constant current testing.

The Ragone plot (Fig. 8) shows that the BCN/MnO<sub>2</sub> system had an energy density of 11.5 Wh/kg while the symmetric AC system was considerably lower at 2.5 Wh/kg. Similarly, the power density of BCN/MnO<sub>2</sub> was also slightly greater than symmetric AC. At 1 kW/kg, BCN/MnO<sub>2</sub> had an energy density of 10 Wh/kg which is almost five times greater than symmetric AC.

#### 4. Discussion

This paper describes a simple approach to make electrode materials for electrochemical capacitors using pyrolysis of a boron/nitrogen containing polymer blended with CTP. The energy densities of the fabricated capacitors are significantly higher than an activated carbon based double layer capacitor. The method does not require any post treatment/processing such as activation or

purification. Polyborazylene was used as the boron/nitrogen precursor and has been shown to be effective at producing BN when pyrolyzed at high temperatures (800–1200 °C) [26–28]. It is also well known that coal tar pitch is a graphitizing precursor which forms polyaromatic mesophases consisting of planar aromatic carbons when pyrolyzed between 500 and 600 °C [29]. Co-pyrolysis of both these precursors would ideally lead to the incorporation of a significant amount of BN in aromatic domains. By mixing the two precursors (1:1, w/w), BCN were produced with more than 10 at% and 14 at% of B and N, respectively. The presence of boron in the precursor helps to stabilize nitrogen atoms in BCN during pyrolysis, allowing for high nitrogen substitution in the carbon. A significant amount of oxygen is seen in BCN even after high temperature pyrolysis. There are very few reports in the literature that demonstrate the incorporation of such high concentrations of heteroatoms in carbon [30,31].

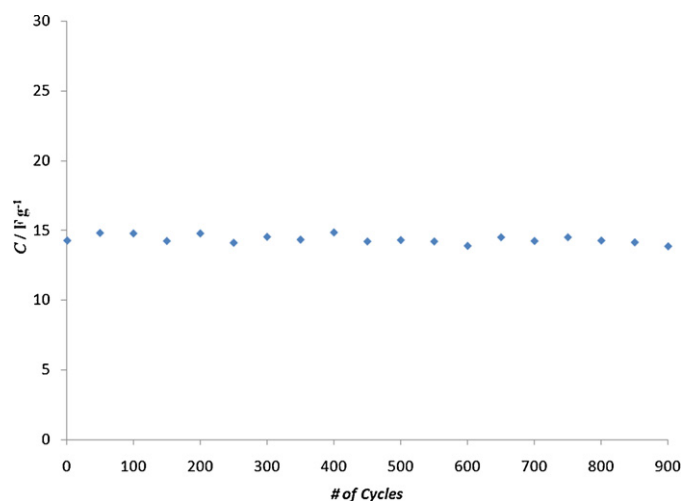


Fig. 7. Cycle life performance of the BCN/MnO<sub>2</sub> capacitor tested using constant current charge/discharge at a load current density of 250 mA/g.

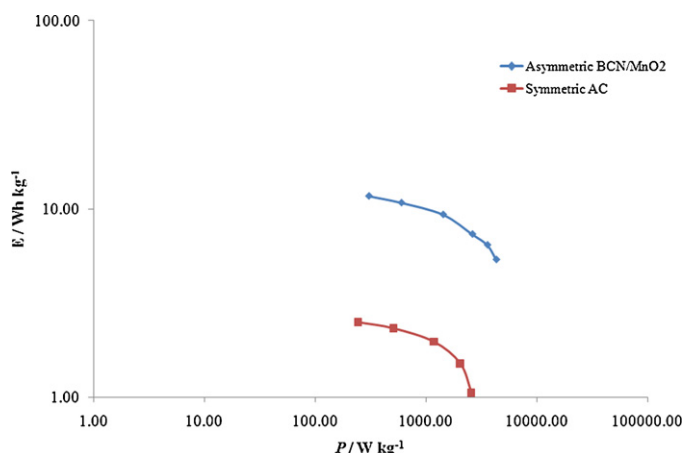
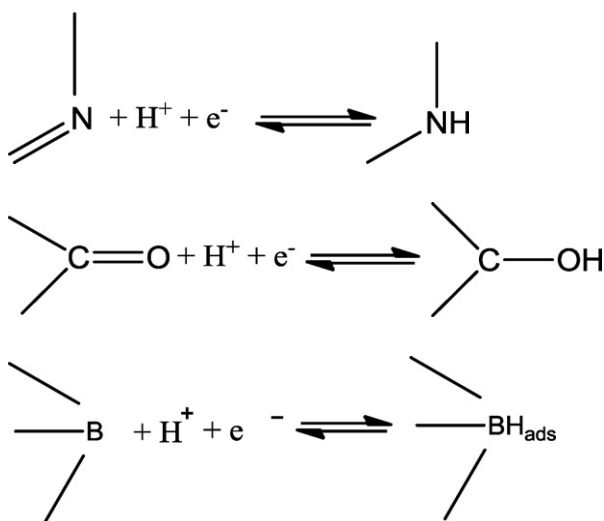
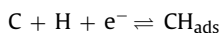


Fig. 8. Ragone plot showing the performance of symmetric AC and asymmetric BCN/MnO<sub>2</sub>.

Recently, Konno et al. showed that it is possible to synthesize BCN with boron content of 5–10% and a surface area of 400 m<sup>2</sup>/g [16]. It was possible to obtain a specific capacitance of 300 F/g (0.75 F/m<sup>2</sup>) in sulfuric acid and 0.3 F/m<sup>2</sup> in neutral electrolytes, respectively. Our results are in agreement with their observations as shown by a specific capacitance of 0.6 F/m<sup>2</sup> in neutral electrolytes. BCN also display a larger electrochemical window ranging from –1.4 V to 1.0 V vs Ag/AgCl as shown in Fig. 3. Such a large electrochemical window in an aqueous system has only been demonstrated in boron doped diamond or nitrogen doped tetrahedral carbon thin films [32–34]. The increased electrochemical window is due to the overpotential that can be applied due to the pseudocapacitive reactions. The key active sites for hydrogen adsorption/redox reactions are polyaromatic carbon, pyridonic N, C–O and B–C in the carbon framework. The possible reactions are as follows:



It is well known that nitrogen and oxygen functional groups can significantly contribute to pseudocapacitance due to favorable reversible redox interaction with protons [10–12]. Boron substituted carbons have been considered as potential hydrogen adsorbents due to the strong interaction of hydrogen with electron deficient boron atoms in the carbon framework [35–37]. The presence of substitutional boron in BCN can play a similar role, resulting in strong electroadsorption of hydrogen atoms

and shifting the hydrogen evolution potential. The large overpotential can also be attributed to the presence of stable redox functional groups that act as a barrier for adsorption/desorption processes inhibiting hydrogen evolution reactions [38]. This phenomenon has been successfully used to extend the cell voltage of the fabricated asymmetric capacitor with excellent cyclability. We envision that improving the surface area of the electrode will substantially increase the energy density of the asymmetric capacitors.

## 5. Conclusion

This paper describes a co-pyrolysis approach to develop BCN electrodes for ultracapacitor applications. The synthesized BCN shows stable pseudocapacitive behavior capable of increasing the overpotential of hydrogen evolution reaction to almost –1.4 V vs Ag/AgCl. The asymmetric capacitor fabricated using BCN/MnO<sub>2</sub> showed an energy density of 10 Wh/kg stable up to 1000 cycles, which is five times more than the symmetric AC system studied. The synthesized BCN could offer significant advantages in terms of volumetric capacitances as well as cost and purity compared to double layer activated carbon electrodes used currently in ultracapacitor technologies.

## Acknowledgements

The authors acknowledge Consortium of Premium Carbon Products from Coal (CPCPC) for providing the funding for this project (Subcontract No. 3556-TPSU-DOE-1874) and Materials Research Institute at the Pennsylvania State University for providing access to characterization facilities.

## References

- [1] L.S. Zhang, *Int. J. Hydrogen Energy* 34 (2009) 4889.
- [2] P. Simon, A.F. Burke, *Electrochem. Soc. Interf.* 17 (2008) 38.
- [3] K. Naoi, M. Morita, *Electrochem. Soc. Interf.* 17 (2008) 44.
- [4] D. Bélanger, T. Brousse, J.W. Long, *Electrochem. Soc. Interf.* 17 (2008) 53.
- [5] S. Sarangapani, B.V. Tilak, C.P. Chen, *Electrochem. Soc. Interf.* 143 (1996) 3791.
- [6] L.L. Zhang, X.S. Zhao, *Chem. Soc. Rev.* 38 (2009) 2520.
- [7] C.J. Xu, H.D. Du, B.H. Li, F.Y. Kang, Y.Q. Zeng, *J. Electrochem. Soc.* 156 (2009) A435.
- [8] C.J. Xu, H.D. Du, B.H. Li, F.Y. Kang, Y.Q. Zeng, *J. Electrochem. Soc.* 156 (2009) A73.
- [9] V. Khomenko, E. Raymundo-Pinero, E. Frackowiak, F. Beguin, *Appl. Phys. A* 82 (2006) 567.
- [10] E. Frackowiak, F. Beguin, *Carbon* 39 (2001) 937.
- [11] M. Kawaguchi, A. Itoh, S. Yagi, H. Oda, *J. Power Sources* 172 (2007) 481.
- [12] F. Beguin, K. Szostak, G. Lota, E. Frackowiak, *Adv. Mater.* 17 (2005) 2380.
- [13] D.-W. Wang, F. Li, Z.-G. Chen, G.Q. Lu, H.-M. Cheng, *Chem. Mater.* 20 (2008) 7195.
- [14] S. Shiraishi, M. Kibe, T. Yokoyama, H. Kurihara, N. Patel, A. Oya, Y. Kaburagi, Y. Hishiyama, *Appl. Phys. A* 82 (2006) 585.
- [15] T. Kwon, H. Nishihara, H. Itoi, Q.-H. Yang, T. Kyotani, *Langmuir* 25 (2009) 11961.
- [16] H. Konno, T. Ito, M. Ushiro, K. Fushimi, K. Azumi, *J. Power Sources* 195 (2010) 1739.
- [17] R. Rajagopalan, K. Perez, H.C. Foley, *Mater. Res. Soc. Symp. Proc.* 973 (2007), 0973-BB07-03.
- [18] T. Tomko, R. Rajagopalan, M. Lanagan, H.C. Foley, *J. Power Sources* (2010), doi:10.1016/j.jpowsour.2010.10.004.
- [19] V. Subramanian, H.W. Zhu, B.Q. Wei, *Chem. Phys. Lett.* 453 (2008) 242.
- [20] H. Konno, H. Oka, K. Shiba, H. Tachikawa, M. Inagaki, *Carbon* 37 (1999) 887.
- [21] H. Konno, K. Shiba, H. Tachikawa, T. Nakahashi, H. Oka, M. Inagaki, *Synth. Met.* 125 (2002) 189.
- [22] K. Stanczyk, R. Dziembaj, Z. Piwowarska, S. Witkowski, *Carbon* 33 (1995) 1383.
- [23] E. Desimoni, G.I. Casella, A. Morone, P.A.M. Sherwood, *Surf. Interf. Anal.* 15 (1990) 627.
- [24] R.J.J. Jansen, H. van Bekkum, *Carbon* 33 (1995) 1021.
- [25] G. Gryglewicz, J. Machnikowski, E. Lorenc-Grabowska, G. Lota, E. Frackowiak, *Electrochim. Acta* 50 (2005) 1197.
- [26] R.I. Wagner, J.L. Bradford, *Inorg. Chem.* 1 (1962) 99.
- [27] P.F. Fazen, E.E. Remsen, J.S. Beck, P.J. Carroll, A.R. McGhie, L.S. Sneddon, *Chem. Mater.* 7 (1995) 1942.

- [28] T. Wideman, P.J. Fazen, K. Su, E.E. Remsen, G.A. Zank, L.G. Sneddon, *Appl. Organomet. Chem.* 12 (1998) 681.
- [29] C. Blanco, R. Santamaria, J. Bermejo, R. Menendez, *Carbon* 38 (2000) 517.
- [30] Y.P. Wu, S.B. Fang, Y.Y. Jiang, *J. Mater. Chem.* 8 (1998) 2223.
- [31] J. Kim, M. Choi, R. Ryoo, *Bull. Korean Chem. Soc.* 29 (2008) 413.
- [32] H.B. Martin, A. Argoitia, U. Landau, A.B. Anderson, J.C. Angus, *J. Electrochem. Soc.* 143 (1996) L133.
- [33] F. Beck, H. Krohn, W. Kaiser, M. Fryda, C.P. Klages, L. Schafer, *Electrochim. Acta* 44 (1998) 525.
- [34] N.C. Yee, Q. Shi, W.-B. Cai, D.A. Scherson, B. Miller, *Electrochem. Solid-State Lett.* 4 (2001) E42.
- [35] T.C.M. Chung, Y. Jeong, Q. Chen, A. Kleinhammes, Y. Wu, *J. Am. Chem. Soc.* 130 (2008) 6668.
- [36] H. Kabbour, T.F. Baumann, J.H. Satcher, A. Saulnier, C.C. Ahn, *Chem. Mater.* 18 (2006) 6085.
- [37] X. Sha, A.C. Cooper, W.H. Bailey III, H. Cheng, *J. Phys. Chem. C* 114 (2010) 3260.
- [38] A. Kapalka, G. Foti, C. Comninellis, *Electrochem. Commun.* 10 (2008) 607.